Dev Genes Evol (1999) 209:349–356

ORIGINAL ARTICLE

David M. Parichy · Michael Stigson · S. Randal Voss

Genetic analysis of *steel* and the PG-M/versican-encoding gene *AxPG* as candidates for the white (*d*) pigmentation mutant in the salamander *Ambystoma mexicanum*

Received: 11 November 1998 / Accepted: 30 January 1999

Abstract Vertebrate non-retinal pigment cells are derived from neural crest (NC) cells, and several mutations have been identified in the Mexican axolotl *Ambystoma mexicanum* (Ambystomatidae) that affect the development of these cell lineages. In "white" (*d*) mutant axolotls, premigratory NC cells differentiate as pigment cells, yet fail to disperse, survive, or both, and this leads to a nearly complete absence of pigment cells in the skin. Previous studies revealed that *d* affects pigment cell development non-autonomously, and have reported differences between white and wild-type axolotls in the structure and composition of the extracellular matrix through which NC and pigment cells migrate. Here we test the correspondence of *d* and two candidate genes: *steel* and *AxPG*. In amniotes, *Steel* encodes the cytokine Steel factor (mast cell growth factor; stem cell factor; kit ligand), which is expressed along the migratory pathways of melanocyte precursors and is required by these cells for their migration and survival; mammalian *Steel* mutants resemble white mutant axolotls in having a deficit or complete absence of pigment cells. In contrast, *AxPG* encodes a PG-M/versican-like proteoglycan that may promote the migration of *A. mexicanum* pigment cells, and AxPG expression is reduced in white mutant axolotls. We cloned a salamander orthologue of *steel* and used a partial genetic linkage map of *Ambystoma* to determine the genomic locations of *steel*, *AxPG*, and *d*. We show that the three genes map to different linkage groups, excluding *steel* and *AxPG* as candidates for *d*.

Key words Pigment cell · Growth factor · Extracellular matrix · Neural crest · Proteoglycan

Edited by D.A. Weisblat

Supplementary material: Additional documentary material has been deposited in electronic form and can be obtained from http://link.springer.de/link/service/journals/00427/index.htm

D.M. Parichy (✉)[1]
Section of Integrative Biology, University of Texas at Austin, Austin TX 78712-1064, USA

M. Stigson[2]
Department of Veterinary Medical Chemistry, Swedish University of Agricultural Sciences, Uppsala, Sweden

S.R. Voss
Department of Biology, Colorado State University, Ft. Collins, CO 80523, USA

Present addresses:
[1] Department of Genetics, Box 8232, Washington University School of Medicine, 4566 Scott Avenue, St. Louis, MO 63110, USA, e-mail: dparichy@genetics.wustl.edu, Tel.: +1-314-362-2733, Fax: +1-314-362-7855
[2] Department of Developmental and Cell Biology, University of California at Irvine, Irvine, CA 92697-2275, USA

Introduction

Pigment cells in the skin of vertebrates are derived from neural crest (NC) cells, which also contribute to the peripheral nervous system, craniofacial skeleton, and many other characters (Groves and Bronner-Fraser 1999; Hall and Hörstadius 1988; Reedy et al. 1998). NC cells arise along the dorsal neural tube shortly after neurulation then disperse widely throughout the embyro, with most of the cells that contribute to externally visible pigment patterns traveling within a dorsolateral migratory pathway between the somite and the epidermis. An understanding of the factors governing the morphogenetic behavior of these cells is essential for understanding the formation of pigment patterns and how these patterns evolve (Parichy 1996a). In the salamander *Ambystoma mexicanum* (the laboratory axolotl; family Ambystomatidae) four spontaneous mutations affecting NC-derived pigment cells have been isolated (Frost et al. 1984). All are recessive and inherited in a simple Mendelian fashion independently of one another. Although three of the mutants appear to have defects primarily in pigment synthesis, the "white" (*d*) mutation (Häcker 1907) affects the morphogenetic behavior of these cells.

The defect associated with the white mutant is apparent by early larval stages. In *A. mexicanum* and other sal-

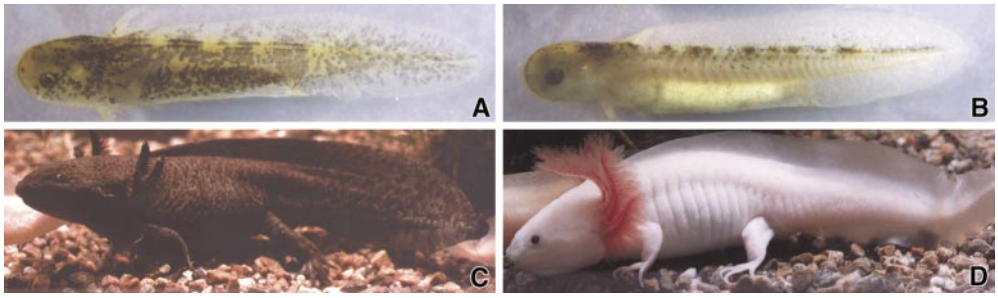

Fig. 1A–D Wild-type (*D/–*) and white mutant (*d/d*) *A. mexicanum*. **A** Hatching (stage 41) wild-type larva displays melanophores and xanthophores covering the flank. **B** Same stage white mutant larva exhibits fewer melanophores and xanthophores, and most are confined to the vicinity of the dorsal myotomes above the neural tube, with few pigment cells further ventrally. **C** Wild-type adult exhibits a dark green and black mottled pattern. **D** White mutant adult completely lacks pigment cells in the skin. Actual size of hatching stage: approx. 12 mm; actual size of adults: approx. 20 cm

amanders, premigratory NC cells form a transient cord immediately dorsal to the neural tube and, while in this position, some of these cells begin to differentiate into either of two types of pigment cell: black melanophores or yellow xanthophores (Epperlein and Löfberg 1993; Löfberg et al. 1980; Parichy 1996a, 1996b). In wild-type *A. mexicanum*, pigment cells and their precursors then disperse into the dorsolateral migratory pathway, and by the stage of first feeding these cells cover most of the trunk (Fig. 1A). In white (*d/d*) mutants, however, most of these cells fail to disperse, and therefore even by early larval stages melanophores and xanthophores remain confined principally to a narrow band along the dorsal myotomes (Keller et al. 1982; Keller and Spieth 1984; Spieth and Keller 1984; Fig. 1B). During later development through adult stages wild-type axolotls develop an irregular green and black mottling (Fig. 1C). In contrast, white axolotls remain devoid of pigmentation as larvae, and most remain completely unpigmented as adults (Fig. 1D), although individuals occasionally develop patches of dark pigmentation after sexual maturity (Frost et al. 1984). The white mutation also results in diminished NC cell proliferation (Dalton and Hall 1950; Hoerter 1977) and fewer NC-derived cells within ganglia of the peripheral nervous system (Borack 1972).

Because of its dramatic phenotype, the cellular bases of the defect in white mutant axolotls have been studied for over 60 years. Together, these studies suggest that *d* acts principally in a non-autonomous manner with respect to NC pigment cell lineages, via the extracellular environment that these cells encounter. For example, embryological grafting experiments revealed that pigment cells of white mutant embryos can populate the flanks of wild-type hosts, whereas wild-type pigment cells fail to populate the flank of white mutant hosts (DuShane 1935, 1939). Subsequent studies identified the epidermis (Bogomolova and Korochkin 1973; Dalton 1949, 1950; Keller et al. 1982) or the subepidermal extracellular matrix (ECM; Löfberg et al. 1989) as the principal site of the defect in the white mutant, and differences in the structure and composition of white and wild-type subepidermal ECMs have been reported (Löfberg et al. 1989; Perris et al. 1990; Spieth and Keller 1984; Stigson 1996). Nevertheless, conflicting results among some of these studies (e.g., Epperlein and Löfberg 1993; Löfberg et al. 1989; Perris et al. 1990), and suggestions that *d* also may act autonomously within NC pigment cell lineages (Thibaudeau and Frost-Mason 1992) have complicated interpretations of the white phenotype. Clearly, further analysis of the roles played by the white gene during pigment pattern development would be facilitated by its identification at the molecular level.

In the present study we test two candidate genes for their correspondence to the white (*d*) locus: *Steel* and *AxPG*. In amniotes, orthologues of *Steel* (*Sl*, *Mgf*) encode the cytokine Steel factor (SLF; also known as mast cell growth factor and stem cell factor), which is the ligand for the transmembrane receptor tyrosine kinase, Kit (Flanagan and Leder 1990; Huang et al. 1990; Martin et al. 1990; Zsebo et al. 1990). Several similarities between the activities of *Steel* and *d* suggest a correspondence of these two genes. For example, *Steel* mutants in mammals have melanocyte deficiencies and white coat coloration, and act principally in a non-autonomous manner relative to cells in the NC melanocyte lineage (Besmer et al. 1993; Mayer and Green 1968). Consistent with these observations, *Steel* in amniotes is expressed by cells in the environment through which pigment cells and their precursors migrate (Lecoin et al. 1995; Matsui et al. 1990; Motro et al. 1991; Wehrle-Haller and Weston 1995; but for *Steel* expression by avian NC cells and possible cell-autonomous activity as well, see Guo et al. 1997). Moreover, SLF acts as a cell membrane-bound form and a soluble form that may associate with ECM, and a *Steel* mutant in mouse exhibits ECM defects (Anderson et al. 1990; Flanagan et al. 1991; Morrison-Graham et al. 1990a, 1990b). Pigment cells and their precursors in both amniotes and teleosts express the SLF receptor, Kit, and signal transduction through Kit promotes the normal migration, proliferation, and survival of these cells (Bernex et al. 1996; Kunisada et al. 1998; Langtimm-Sedlak et al. 1996; Lecoin et al. 1995; MacKenzie et al. 1997; Murphy et al. 1992; Reid et al. 1995; Wehrle-Haller and Weston 1995; Parichy et al., in preparation). SLF also supports the survival of NC-de-

rived cells within ganglia of the peripheral nervous system (Hirata et al. 1993). Finally, although *Steel* has not been cloned to date from any ectothermic vertebrate, mutations in the zebrafish orthologue of *Kit* yield phenotypes that resemble white axolotls even more closely than amniote mutants: larval melanophores differentiate but fail to disperse properly and ultimately die; a new population of melanophores subsequently differentiates during the larval-to-adult transition (Parichy et al., in preparation). Whereas *Steel* and *Kit* mutants in mouse typically have pleiotropic effects on hematopoiesis and gametogenesis (Besmer et al. 1993), even null alleles of zebrafish *kit* have effects limited to pigmentation. Taken together these observations make *Steel* a strong candidate for *d*.

Previous studies also suggest potential allelism of *AxPG* and *d*. *A. mexicanum AxPG* encodes the core protein of an extremely high molecular weight chondroitin/dermatan sulfate proteoglycan (CSPG) and is orthologous to amniote genes encoding PG-M/versican (Stigson 1996; Stigson et al. 1997a), which is suggested to facilitate cell migration by virtue of its antiadhesive properties (Morris-Kay and Tuckett 1989; Yamagata et al. 1989; see also Erickson and Perris 1993; Wight et al. 1992). In axolotls the product of *AxPG*, which we refer to simply as PG-M/versican, forms very large disulfide-stabilized complexes (Stigson and Kjellén 1991) and is the predominant CSPG found in the subepidermal ECM during NC and pigment cell migration (Stigson et al. 1997a). Intriguingly, white mutant axolotls exhibit both reduced expression of *AxPG* mRNA in the epidermis (Stigson et al. 1997b), and diminished levels of CSPG in the subepidermal ECM as determined by ultrastructural methods (Keller and Spieth 1984; Löfberg et al. 1989; Perris et al. 1990; Spieth and Keller 1984). These observations raise the possibility that changes in *AxPG* expression are causally related to the development of the white phenotype, and suggest the hypothesis that *AxPG* might itself correspond to the *d* locus (e.g., the *d* lesion might be found in an upstream regulatory element of *AxPG*, or might destabilize AxPG mRNA, resulting in diminished *AxPG* activity). Here we use genetic linkage mapping to test both *A. mexicanum steel* and *AxPG* as candidates for *d*.

Materials and methods

Cloning and analysis of *A. mexicanum steel*

Total RNA from wild-type (*D/–*) *A. mexicanum* embryos was isolated using a Total RNA Maxi Kit (Qiagen, Chatsworth, Calif., USA) and polyA mRNA was selected using an Oligotex mRNA Mini Kit (Qiagen). First-strand cDNA was synthesized with Superscript II reverse transcriptase (Life Technologies, Grand Island, N.Y., USA) and primed with random hexamers. This cDNA was diluted tenfold and 0.5 µl was used in a 25-µl polymerase chain reaction (PCR) with consensus primers designed from mammalian and avian *Steel* cDNAs [stlCf: 5′–AGACACAAACTTGGATTATCAC–3′; stlCr: 5′–GG(A/C/T)TGT(G/T)TCTTCTTCCAGTAT–3′] at an annealing temperature of 50°C. This PCR was then diluted and reamplified, yielding a single visible 660 bp fragment that was gel purified, subcloned into pCRII (Invitrogen, Carlsbad, Calif., USA), and sequenced.

To isolate the 5′ and 3′ ends of *A. mexicanum steel* mRNA, we used a RACE procedure and the Marathon cDNA Amplification Kit (Clontech, Palo Alto, Calif., USA). We constructed a RACE cDNA library from stage 35 (Bordzilovskaya et al. 1989) *A. mexicanum* embryos and used outward directed primers (see "Supplementary Information") with Clontech RACE adaptor primer AP1 to amplify overlapping 5′ and 3′ RACE products that we subcloned and sequenced. We isolated two 5′ RACE clones (one extending 6 bp further 5′ than the other), and three identical 3′ RACE clones. We then used these sequences to design primers (stlFLf: 5′–GCAGGTCAAGGAACCGAGGCGGACAG–3′; stlFLr: 5′–TTTGGGGGTGAGATTTTGTTTATTTTCACACAAAGA–3′) for amplifying a single presumptive *steel* cDNA from the RACE library. The resulting product was subcloned into pKRX (Schutte et al. 1997) and sequenced with an ABI 377 automated sequencer and AmpliTaq FS dye terminator sequencing chemistry (Perkin Elmer, Norwalk, Conn., USA). Multiple continuous and overlapping reads were obtained for a single clone of *A. mexicanum steel* cDNA and these sequences were verified and found to be identical to three complete sequences that were obtained from independent amplifications of stage 35 and stage 41 first-strand cDNAs using reverse transcriptase PCR. All sequence analyses were performed using GCG software (Genetics Computer Group, Madison, Wis., USA).

steel expression was examined by northern blotting. Total RNA was isolated using Trizol reagent (Life Technologies) and precipitated with an equal volume 8 M LiCl, 5 mM EDTA. After washing with 70% ethanol, the pellets were resuspended and concentrations determined spectrophotometrically. A quantity of 20 µg total RNA was size-separated by electrophoresis in a denaturing agarose/formaldehyde/3-(4-Morpholino)propanesulfonic acid gel and equal loading among samples was assessed by UV shadowing of the 18S and 28S ribosomal subunits. Gels were blotted (Chomczynski 1992) for 2 h onto Hybond N+ nylon membrane (Amersham, Uppsala, Sweden). Asymmetric PCR was then used to generate a ^{32}P-labeled DNA probe from linearized vector containing the original *steel* fragment (from degenerate PCR) and hybridization was carried out at 60°C in Church-Gilbert hybridization solution (Sagerström and Sive 1996). After stringency washes, autoradiographs were exposed for 18–48 h before developing.

Genetic linkage mapping

To map the relative locations of *d*, *steel*, and *AxPG*, we used a partial genetic linkage map of *Ambystoma*. This map is based upon a crossing design that was described previously (Voss 1995). Briefly, an interspecific cross was made between a female *A. tigrinum tigrinum* and a male *A. mexicanum* (P1 generation). The male *A. mexicanum* was a known carrier of the recessive white allele (genotype: D_{mex}/d); we assume the genotype of the *A. t. tigrinum* female to be D_{tig}/D_{tig}. Several F1 male hybrids were backcrossed to female *A. mexicanum* (D_{mex}/d) and two crosses (crosses 3 and 4 in Voss 1995) that segregated the white phenotype (paternal hybrid genotype: D_{tig}/d) were used for mapping. Offspring were scored for pigmentation phenotype, and the genomic location of *d* was mapped by bulked segregant analysis to a local map of randomly amplified polymorphic DNA (RAPD) markers (Voss and Shaffer 1996). Subsequently, *d* was integrated into a more comprehensive, yet partial genetic linkage map of amplified fragment length polymorphism (AFLP) markers (Voss and Shaffer 1997) using Mapmaker 3.0b (Lander et al. 1987) and a critical LOD threshold of 3.0. Because wild-type and white coloration were segregating as F2 markers (3:1) in the backcross, the position of *d* was determined by considering only the genotypic scores of white individuals, and confirmed by maximum likelihood estimation using the entire mapping panel (Voss, unpublished data).

steel and *AxPG* were mapped by scoring the segregation of polymorphic alleles among backcross offspring. For *steel*, we

designed PCR primers (stlI3f: 5′–ACCTCCCAAGTGACTACAGTATATC-3′; stlI3r: 5′–GGCTGTTAGACACTTTGTGAACCAT–3′) to amplify across the predicted location of intron 3, based on comparison with mouse (Bedell et al. 1996). Sequencing the resulting approx. 1200 bp fragment revealed several polymorphisms between *A. mexicanum* and *A. t. tigrinum*. For linkage mapping, we designed a new reverse primer (stlI3rb: 5′–ACCTCCCACTCAAACAGCTTC-3′) located 207 bp from the 5′ end of the intron and used this in conjunction with stlI3f to amplify 263 bp fragments from genomic DNA that we scored by single strand conformational polymorphism (SSCP) on 7% polyacrylamide gels (Hongyo et al. 1993). For *AxPG* we designed PCR primers (AxPGf: 5′–GACAGCAGTGGAGACAGATGAAGAAC–3′; AxPGr: 5′–TCTACAGCGACGGGAGATGACG–3′) to amplify within the exon coding for a unique chondroitin sulfate-attachment domain (Stigson 1996; Stigson et al. 1997a). We used these primers to amplify 708 bp fragments from genomic DNAs of *A. mexicanum* and *A. t. tigrinum*. *A. mexicanum* alleles exhibited a unique *Rsa*I site that we used for scoring individuals in the mapping crosses.

Results and discussion

Cloning and analysis of an *A. mexicanum steel* cDNA

To test the correspondence of *steel* and *d* we first cloned an *A. mexicanum steel* cDNA. We isolated overlapping 5′ and 3′ RACE products totaling 2139 bp then used internal primers to amplify and clone a 2083 bp cDNA containing an open reading frame (ORF) of 813 bp (for annotated sequence, see "Supplementary Data"; GenBank accession number: AF119044). Searches of protein and nucleotide databases by BLAST identified this cDNA as an orthologue of amniote *Steel*, hence we designate the *A. mexicanum* gene encoding this mRNA *steel*. Because the 5′ untranslated region (UTR) of *A. mexicanum steel* mRNA is the longest of any species yet identified (273 bp), we infer that we have isolated a full length or nearly full length *steel* cDNA. Table 1 presents nucleotide sequence identities within the ORFs of *steel* orthologues. Although sequence identities within birds and mammals are at least 87%, identities across vertebrate classes are considerably lower. Avian and mammalian ORFs share on average 68% nucleotide identity, whereas *A. mexicanum steel* shares on average 53% and 58% nucleotide identity with avian and mammalian sequences, respectively; a UPGMA phenogram (Sneath and Sokal 1973) places the *A. mexicanum steel* sequence basal to amniote *Steel* sequences (not shown). Average amino acid similarities of *A. mexicanum* SLF with avian and mammalian SLFs are 46% and 49%, respectively (Table 1). Conserved amino acids, including four cysteine residues, are scattered throughout the *A. mexicanum steel* gene product (Fig. 2), and hydrophilicity plots (not shown) reveal putative signal and transmembrane domains corresponding to those of mammalian and avian SLFs.

Table 1 Sequence similarities and identities of *Steel* orthologues within cDNA open reading frames [*above diagonal* percentage amino acid similarities (*upper*) and identities (*lower*), *below diagonal* percentage nucleotide identities] (amniote *Steel* sequences from: Bedell et al. 1996; Petitte and Kulik 1996; Zhang and Anthony 1994; Zhou et al. 1993; Dunham and Onions, direct submission, GenBank Accession no. D50833)

	Axolotl	Chicken	Quail	Mouse	Pig	Cat
Axolotl	–	49 42	49 42	50 40	45 38	43 36
Chicken	58	–	98 98	64 57	62 54	60 53
Quail	57	97	–	63 56	62 53	59 52
Mouse	53	69	69	–	85 82	84 81
Pig	53	68	68	87	–	94 92
Cat	52	67	67	87	93	–

In amniotes, two forms of SLF are produced by differential mRNA splicing (Anderson et al. 1990; Flanagan et al. 1991; Huang et al. 1992; Majumdar et al. 1994). A longer transcript produces a protein with a serine protease cleavage site containing several small amino acids that are highly conserved among birds and mammals (PPVA↓A↓SS; Fig. 2); cleavage at this site yields a soluble form of SLF that is released from the cell membrane. In contrast, an approx. 80 nucleotide (nt) shorter transcript (lacking exon 6) generates a protein without this cleavage site that remains preferentially associated with the cell surface. Although both membrane-bound and soluble SLF exhibit biological activity, their effects on target cell populations may differ (e.g., Tajima et al. 1998; Toksoz et al. 1992). For example, both forms stimulate NC migration, but only membrane-bound SLF supports the maintenance of these cells after their initial dispersal (Wehrle-Haller and Weston 1995). The *A. mexicanum steel* cDNA we have isolated corresponds to the longer transcript of amniotes. Nevertheless, the major serine protease cleavage site is not well conserved (FSFMPSS), nor are two additional motifs that may identify alternative sites of protease cleavage (Longley et al. 1997; Majumdar et al. 1994; Fig. 2). We have not been able to identify a smaller splice variant of *A. mexicanum steel* mRNA by northern blot analysis (see below), or repeated attempts at PCR amplification using a variety of primer sets to the *steel* ORF and cDNAs from embryonic stages and various adult tissues. Although biochemical studies are required to address definitively whether or not *A. mexicanum* SLF is processed proteolytically (e.g., Cheng and Flanagan 1994), the present observations raise the possibility that *A. mexicanum* may produce only a membrane-bound form of SLF, perhaps reflecting evolutionary divergence between amniotes and amphibians in *steel* function.

Interestingly, sequence analysis of the 5′ UTR of *A. mexicanum steel* cDNA raises the possibility of translational regulation of *steel* expression. The 5′ UTRs of amniote *Steel* cDNAs include two conserved ATGs upstream of the initiator methionine (at positions –110 and –75 nt relative to the start codon in mouse) and the region extending from the first of these ATGs to the initiator methionine is very similar across species (e.g., 79%

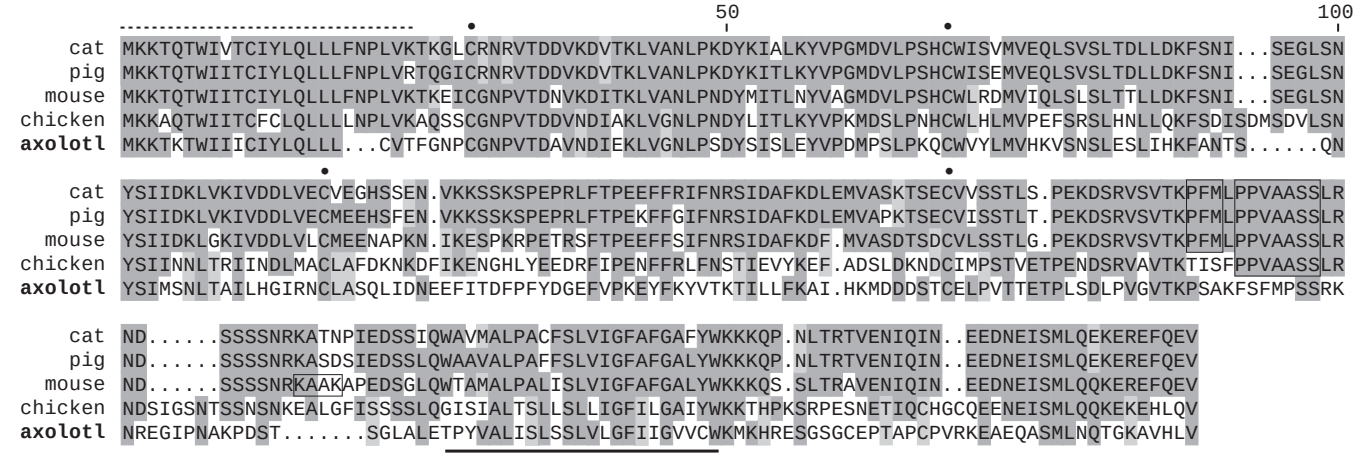

Fig. 2 Alignments of deduced amino acid sequences for SLF of amniotes and *A. mexicanum* (Bedell et al. 1996; Zhang and Anthony 1994; Zhou et al. 1993; Dunham and Onions, GenBank accession no. D50833). *Dark gray shading* residues conserved across multiple species; *light gray shading* residues conserved across fewer species; two alternative residues shared equally among species are arbitrarily *shaded dark* or *light*. • Cysteines conserved across all five species. Also indicated are putative signal sequences (…) and transmembrane domains (—). Protease cleavage sites are *boxed*

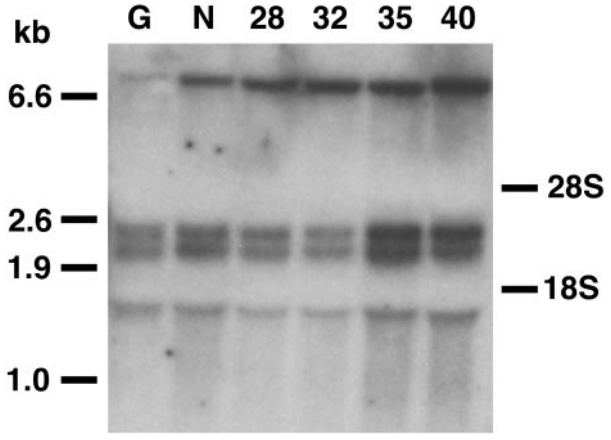

Fig. 3 Expression of *A. mexicanum steel* RNA. *steel* expression was examined by northern blot of total RNA isolated from gastrula through hatching stages (*indicated above lanes*; *G* gastrula, stages 10–12; *N* neural plate and neural fold closure, stages 15–17; stages 32–35 correspond to the period of NC and pigment cell migration in the trunk; stage 40 is a free-swimming hatchling; Bordzilovskaya et al. 1989; Löfberg et al. 1980). Three major transcripts are observed at each stage (see text for details). An additional band immediately below the position of the 18S rRNA subunit probably is artifactual

nucleotide identity between mouse and chicken; for details see Bedell et al. 1996). Such upstream ORFs are known to modulate both the efficiency and tissue specificity of translation in other systems (Kozak 1991; Zimmer et al. 1994). Comparison of the 110 nt region preceding the initiator methionine in *A. mexicanum steel* reveals nucleotide identities of 62% and 55% with mouse and chicken, respectively, similar to values observed for the *steel* ORF. The 5′ UTR of *A. mexicanum steel* lacks an ATG corresponding to the –110 ATG of mouse, but a novel ATG is present in frame and immediately downstream at position –92; translation of this ORF would produce a 31 amino acid polypeptide, with a stop codon overlapping the initiator methionine, which is true of amniotes as well. The ATG at –75 nt is present in *A. mexicanum*; translation from this site would yield a 7 amino acid polypeptide. As in amniotes, none of the three ATGs is in a sequence context that is optimal for translation initiation (Kozak 1991). The deep phylogenetic conservation of elements within the 5′ UTR strongly suggests they have consequences for *steel* function or expression, although this has yet to be tested directly. The finding of an mRNA instability motif (Zubiaga et al. 1995) in the 1050 nt 3′ UTR of *A. mexicanum steel* cDNA also is consistent with post-transcriptional regulation of *steel* expression.

To determine when *steel* is expressed, we examined northern blots of total RNA isolated from wild-type *A. mexicanum* during and prior to larval pigment pattern formation. Three transcripts were detected of approx. 2.1, approx. 2.2, and greater than 6.6 kb from gastrula through hatching stages (Fig. 3). We infer that the smallest of these corresponds to a presumably full length 2139 nt mRNA (see “Supplementary Data”). Since PCR of the *steel* ORF from embryonic and adult cDNAs also amplified a slightly larger fragment, possibly corresponding to the approx. 2.2 kb band identified by northern blot, we subcloned and sequenced this fragment. These analyses revealed a 68 nt insert in the ORF at a position that corresponds to the location of intron 1 in mouse. Thus we infer that the approx. 2.2 kb fragment identified by northern analysis of total RNA may represent incompletely processed transcript. The greater than 6.6 kb fragment also may represent precursor RNA.

Genetic mapping of *d*, *steel*, and *AxPG*

We mapped *steel* and *AxPG* relative to 242 AFLP markers, 3 RAPDs, and *d* segregating in a 44 individual map-

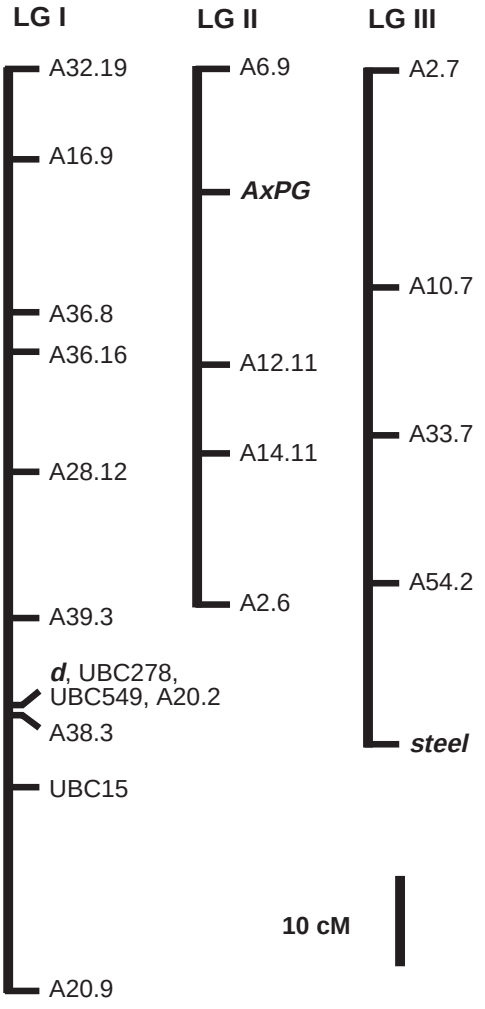

Fig. 4 Map positions of *d*, *steel*, and *AxPG*. The three genes map to different provisional linkage groups, demonstrating that neither candidate gene corresponds to *d*

ping panel. Linkage analysis with a default linkage criterion of LOD=3.0 identified 48 provisional linkage groups (LGs; the haploid chromosome number of *A. mexicanum* is 14; Callan 1966). Given that the inheritence of white coloration in these crosses is consistent with a single genetic factor, *d* (Voss 1995; Voss and Shaffer 1996), *steel* or *AxPG* would be expected to map to the same location as *d* if a lesion in either gene were responsible for the white phenotype. However, *d*, *steel*, and *AxPG* all mapped to different linkage groups: *d* mapped to provisional LG I, *steel* mapped to a distal position on LG III, and *AxPG* mapped to LG II (Fig. 4). Even if LG I were joined with LG II or LG III by a denser set of genetic markers, the failure of *d* to segregate with *steel* or *AxPG* demonstrates a lack of correspondence among these loci. Accordingly, these data exclude the hypothesis that either *steel* or *AxPG* is allelic to *d*.

Conclusion

steel and *AxPG* represented the best known candidate genes for *d.* Nevertheless, studies of amniotes suggest several additional candidates, such as endothelins (Lecoin et al. 1998; Reedy et al. 1998), in which lesions in *A. mexicanum* might be responsible for the white defect. Recent mutant screens also have identified a host of mutants that affect pigment pattern development in zebrafish, some of which (in addition to *kit*) cause the disappearance of pigment cells after they have differentiated (Kelsh et al. 1996). These genes also may be reasonable candidates for *d*, but with few exceptions (Parichy et al., in preparation), they remain to be identified at the molecular level. Finally, the altered expression of *AxPG* in *d/d* mutant embryos (Stigson et al. 1997b) and the lack of correspondence of these loci demonstrated in this study imply that the *d* gene product directly or indirectly influences *AxPG* expression. Thus, several genes known to act upstream of PG-M/versican-encoding genes in other systems also are candidates for *d*. For example, transforming growth factor-β and platelet-derived growth factor up-regulate PG-M/versican expression and also promote cell motility (Ataliotis and Mercola 1997; Delannet and Duband 1992; Schönherr et al. 1991). Nevertheless, complex interdependencies in the expression of various ECM components (e.g., Tsukahara et al. 1991) hinders the identification of candidate genes based on functional studies of ECM. Construction of an increasingly dense *A. mexicanum* genetic linkage map and comparison of synthenic regions across species (Postlethwait et al. 1998) may suggest previously unsuspected candidates, and also should provide an opportunity for identifying *d* using chromosome walking methods.

Acknowledgements This research was supported by NSF IBN-9423116 and NSF-Sloan DBI-9750006 to D.M.P. and NSF BSR-9101128 and NSF IBN-9509802 to S.R.V. D.M.P. thanks C.A. Erickson (University of California at Davis) for support (NIH GM53258), M.S. thanks P. Hakanssons Stiftelse for a Druvan postdoctoral scholarship, and S.R.V. thanks D. Heckel (Clemson University) and H.B. Shaffer (University of California at Davis) for advice and support. The Indiana University Axolotl Colony (Bloomington, Ind.) supplied *A. mexicanum* embryos, and J. Löfberg kindly provided the photographs in Fig. 1.

References

Anderson DM, Lyman SD, Baird A, Wignall JM, Eisenman J, Rauck C, March CJ, Boswell HS, Gimpel SD, Cosman D, Williams DE (1990) Molecular cloning of mast cell growth factor, a hematopoietin that is active in both membrane bound and soluble forms. Cell 63:235–243

Ataliotis P, Mercola M (1997) Distribution and functions of platelet-derived growth factors and their receptors during embryogenesis. Int Rev Cytol 172:95–127

Bedell MA, Copeland NG, Jenkins NA (1996) Multiple pathways for *Steel* regulation suggested by genomic and sequence analysis of the murine *Steel* gene. Genetics 142:927–934

Bernex F, De Sepulveda P, Kress C, Elbaz C, Delouis C, Panthier J-J (1996) Spatial and temporal patterns of c-*kit*-expressing cells in $W^{lacZ}/+$ and W^{lacZ}/W^{lacZ} mouse embryos. Development 122:3023–3033

Besmer P, Manova K, Duttlinger R, Huang EJ, Packer A, Gyssler C, Bachvarova RF (1993) The *kit*-ligand (steel factor) and its receptor c-*kit*/*W*: pleiotropic roles in gametogenesis and melanogenesis. Development 1993 [Suppl]:125–137

Bogomolova VI, Korochkin LI (1973) Development of pigmentation after transplantation of presumptive epidermis between embryos of white axolotls *Ambystoma mexicanum* of different ages. Ontogenez 4:420–424

Borack LI (1972) Gene action on proliferation and migration in the developing neural crest of black and white axolotls, *Ambystoma mexicanum* Shaw. J Exp Zool 179:289–298

Bordzilovskaya NP, Detlaff TA, Duhon ST, Malacinski GM (1989) Developmental-stage series of axolotl embryos. Oxford University Press, Oxford

Callan HG (1966) Chromosomes and nucleoli of the axolotl, *Ambystoma mexicanum*. J Cell Sci 1:85–108

Cheng H-W, Flanagan JG (1994) Transmembrane kit ligand cleavage does not require a signal in the cytoplasmic domain and occurs at a site dependent on spacing from the membrane. Mol Biol Cell 5:943–953

Chomczynski P (1992) One-hour downward alkaline capillary transfer for blotting of DNA and RNA. Anal Biochem 201: 134–139

Dalton HC (1949) Developmental analysis of genetic differences in pigmentation in the axolotl. Proc Natl Acad Sci USA 35:277–283

Dalton HC (1950) Inhibition of chromatoblast migration as a factor in the development of genetic differences in pigmentation in white and black axolotls. J Exp Zool 115:151–170

Dalton HC, Hall J (1950) Gene action in the axolotl. Carnegie Inst Wash Year Book 49:181–188

Delannet M, Duband J-L (1992) Transforming growth factor-β control of cell-substratum adhesion during avian neural crest cell emigration in vitro. Development 116:275–287

DuShane GP (1935) An experimental study of the origin of pigment cells in Amphibia. J Exp Zool 72:1–31

DuShane GP (1939) The role of embryonic ectoderm and mesoderm in pigment production in amphibia. J Exp Zool 82:193–217

Epperlein HH, Löfberg J (1993) The development of the neural crest in amphibians. Ann Anat 175:483–499

Erickson CA, Perris R (1993) The role of cell-cell and cell-matrix interactions in the morphogenesis of the neural crest. Dev Biol 159:60–74

Flanagan JG, Leder P (1990) The *kit* ligand: a cell surface molecule altered in Steel mutant fibroblasts. Cell 63:185–194

Flanagan JG, Chan DC, Leder P (1991) Transmembrane form of the *kit* ligand growth factor is determined by alternative splicing and is missing in the Sl^d mutant. Cell 64:1025–1035

Frost SK, Briggs F, Malacinski GM (1984) A color atlas of pigment genes in the Mexican axolotl (*Ambystoma mexicanum*). Differentiation 26:182–188

Groves AK, Bronner-Fraser M (1999) Neural crest diversification. Curr Top Dev Biol 43:221–258

Guo CS, Wehrle-Haller B, Rossi J, Ciment G (1997) Autocrine regulation of neural crest cell development by Steel factor. Dev Biol 184:61–69

Häcker V (1907) Uber Mendelschen Vererbung bei Axolotln. Zool Anz 31:99–102

Hall BK, Hörstadius S (1988) The neural crest. Oxford University Press, Oxford

Hirata T, Morii E, Morimoto M, Kasugai T, Tsujimura T, Hirota S, Kanakura Y, Nomura S, Kitamura Y (1993) Stem cell factor induces outgrowth of c-*kit*-positive neurites and supports the survival of c-*kit*-positive neurons in dorsal root ganglia of mouse embryos. Development 119:49–56

Hoerter JD (1977) Dosage effects of the white (*d*) and melanoid (*m*) genes on pigment pattern development in the Mexican axolotl, *Ambystoma mexicanum*, Shaw. Dev Biol 59:249–254

Hongyo T, Buzard GS, Calvert RJ, Weghorst CM (1993) 'Cold SSCP': a simple, rapid and non-radioactive method for optimized single-strand conformation polymorphism analyses. Nucleic Acids Res 21:3637–3642

Huang E, Nocka K, Beier DR, Chu T-Y, Buck J, Lahm H-W, Wellner D, Leder P, Besmer P (1990) The hematopoietic growth factor KL is encoded by the *Sl* locus and is the ligand of the c-*kit* receptor, the gene product of the *W* locus. Cell 63:225–233

Huang EJ, Nocka KH, Buck J, Besmer P (1992) Differential expression and processing of two cell associated forms of the Kit-ligand: KL-1 and KL-2. Mol. Biol Cell 3:349–362

Keller RE, Spieth J (1984) Neural crest cell behavior in white and dark larvae of *Ambystoma mexicanum*: time-lapse cinemicrographic analysis of pigment cell movement in vivo and in culture. J Exp Zool 229:109–126

Keller RE, Löfberg J, Spieth J (1982) Neural crest cell behavior in white and dark embryos of *Ambystoma mexicanum*: epidermal inhibition of pigment cell migration in the white axolotl. Dev Biol 89:179–195

Kelsh RN, Brand M, Jiang Y-J, Heisenberg C-P, Lin S, Haffter P, Odenthal J, Mullins MC, van Eeden FJM, Furutani-Seiki M, Granato M, Hammerschmidt M, Kane DA, Warga RM, Beuchle D, Vogelsang L, Nusslein-Volhard C (1996) Zebrafish pigmentation mutations and the processes of neural crest development. Development 123:369–389

Kozak M (1991) An analysis of vertebrate mRNA sequences: intimations of translational control. J Cell Biol 115:887–903

Kunisada T, Yoshida H, Yamazaki H, Miyamoto A, Hemmi H, Nishimura E, Shultz LD, Nishikawa S-I, Hayashi S-I (1998) Transgene expression of steel factor in the basal layer of epidermis promotes survival, proliferation, differentiation and migration of melanocyte precursors. Development 125:2915–2923

Lander ES, Green P, Abrahamson J, Barlow A, Daly MJ, Lincoln SE, Newburg L (1987) MAPMAKER: an interactive computer package for constructing primary genetic linkage maps of experimental and natural populations. Genomics 1:174–181

Langtimm-Sedlak CJ, Schroeder B, Saskowski JL, Carnahan JF, Sieber-Blum M (1996) Multiple actions of stem cell factor in neural crest differentiation in vitro. Dev Biol 174:345–359

Lecoin L, Lahav R, Martin FH, Teillet M-A, Le Douarin NM (1995) *Steel* and *c-kit* in the development of avian melanocytes: a study of normally pigmented birds and of the hyperpigmented mutant silky fowl. Dev Dyn 203:106–118

Lecoin L, Sakurai T, Ngo M-T, Abe Y, Yanagisawa M, Le Douarin NM (1998) Cloning and characterization of a novel endothelin receptor subtype in the avian class. Proc Natl Acad Sci USA 95:3024–3029

Löfberg J, Ahlfors K, Fällström C (1980) Neural crest cell migration in relation to extracellular matrix organization in the embryonic axolotl trunk. Dev Biol 75:148–167

Löfberg J, Perris R, Epperlein HH (1989) Timing in the regulation of neural crest cell migration: retarded "maturation" of regional extracellular matrix inhibits pigment cell migration in embryos of the white axolotl mutant. Dev Biol 131:168–181

Longley BJ, Tyrrell LA, Ma Y, Williams DA, Halaban R, Langley K, Lu HS, Schechter NM (1997) Chymase cleavage of stem cell factor yields a bioactive, soluble product. Proc Natl Acad Sci USA 94:9017–9021

MacKenzie MAF, Jordan SA, Budd PS, Jackson IJ (1997) Activation of the receptor tyrosine kinase Kit is required for the proliferation of melanoblasts in the mouse embryo. Dev Biol 192:99–107

Majumdar MK, Feng L, Medlock E, Toksoz D, Williams DA (1994) Identification and mutation of primary and secondary proteolytic cleavage sites in murine stem cell factor cDNA yields a biologically active, cell associated protein. J Biol Chem 269:1237–1242

Martin FH, Suggs SV, Langley KE, Lu HS, Ting J, Okino KH, Morris CF, McNiece IK, Jacobsen FW, Mendiaz EA, Birkett NC, Smith KA, Johnson MJ, Parker VP, Flores JC, Patel AC, Fisher EF, Erjavec HO, Herrera CJ, Wypych J, Sachdev RK, Pope JA, Leslie I, Wen D, Lin CH, Cupples RL, Zsebo KM (1990) Primary structure and functional expression of rat and human stem cell factor DNAs. Cell 63:203–211

Mason KA, Parker NB, Parichy DM, Voss SR (1998) Molecular characterization of c-*kit* from the Mexican axolotl. Pigment Cell Res 11:175

Matsui Y, Zsebo KM, Hogan LM (1990) Embryonic expression of a haematopoietic growth factor encoded by the *Sl* locus and the ligand for c-kit. Nature 347:667–669

Mayer TC, Green MC (1968) An experimental analysis of the pigment defect caused by mutations at the *W* and *Sl* loci in mice. Dev Biol 18:62–75

Morris-Kay G, Tuckett F (1989) Immunohistochemical localisation of chondroitin sulphate proteoglycans and the effects of chondroitinase ABC in 9- to 11-day rat embryos. Development 106:787–798

Morrison-Graham K, Bork T, Weston JA (1990a) Association between collagen and glycosaminoglycans is altered in dermal extracellular matrix of fetal *Steel* (Sl^d/Sl^d) mice. Dev Biol 139:308–313

Morrison-Graham K, West-Johnsrud L, Weston JA (1990b) Extracellular matrix from normal but not Steel mutant mice enhances melanogenesis in cultured mouse neural crest cells. Dev Biol 139:299–307

Motro B, van der Kooy D, Rossant J, Reith A, Bernstein A (1991) Contiguous patterns of c-*kit* and *steel* expression: analysis of mutations at the *W* and *Sl* loci. Development 113:1207–1221

Murphy M, Reid K, Williams DE, Lyman SD, Bartlett PF (1992) Steel factor is required for maintenance, but not differentiation, of melanocyte precursors in the neural crest. Dev Biol 153:396–401

Ostberg CO, Zhu P, Wight TN, Qwarnström EE (1995) Fibronectin attachment is permissive for IL-1 mediated gene regulation. FEBS Lett 367:93–97

Parichy DM (1996a) Pigment patterns of larval salamanders (Ambystomatidae, Salamandridae): the role of the lateral line sensory system and the evolution of pattern-forming mechanisms. Dev Biol 175:265–282

Parichy DM (1996b) Salamander pigment patterns: how can they be used to study developmental mechanisms and their evolutionary transformation? Int J Dev Biol 40:871–884

Perris R, Löfberg J, Fällström C, von Boxberg Y, Olsson L, Newgreen DF (1990) Structural and compositional divergencies in the extracellular matrix encountered by neural crest cells in the white mutant axolotl embryo. Development 109:533–551

Petitte JN, Kulik MJ (1996) Cloning and characterization of cDNAs encoding two forms of avian stem cell factor. Biochim Biophys Acta 1307:149–151

Postlethwait JH, Yan YL, Gates MA, Horne S, Amores A, Brownlie A, Donovan A, Egan ES, Force A, Gong Z, Goutel C, Fritz A, Kelsh R, Knapik E, Liao E, Paw B, Ransom D, Singer A, Thomson M, Abduljabbar TS, Yelick P, Beier D, Joly JS, Larhammar D, Rosa F, Westerfield M, Zon LI, Johnson SL, Talbot WS (1998) Vertebrate genome evolution and the zebrafish gene map. Nat Genet 18:345–349

Reedy MV, Parichy DM, Erickson CA, Mason KA, Frost-Mason SK (1998) The regulation of melanoblast migration and differentiation. In: Nordland JJ, Boissy RE, Hearing VJ, King RA, Ortonne JP (eds) The pigmentary system: physiology and pathophysiology. Oxford University Press, Oxford, pp 75–95

Reid K, Nishikawa SI, Bartlett PF, Murphy M (1995) Steel factor directs melanocyte development in vitro through selective regulation of the number of of c-kit$^+$ progenitors. Dev Biol 169:568–579

Sagerström CG, Sive H (1996) RNA blot analysis. In: Krieg PA (ed) A laboratory guide to RNA: isolation, analysis, and synthesis. Wiley, New York, pp 83–104

Schönherr E, Järveläinen HT, Sandell LJ, Wight TN (1991) Effects of platelet-derived growth factor and transforming growth factor-β1 on the synthesis of a large versican-like chondroitin sulfate proteoglycan by arterial smooth muscle cells. J Biol Chem 266:17640–17647

Schutte BC, Ranade K, Pruessner J, Dracopoli N (1997) Optimized conditions for cloining PCR products into an *Xcm*I T-vector. Biotechniques 22:40–44

Sneath PHA, Sokal RR (1973) Numerical taxonomy. Freeman, San Francisco

Spieth J, Keller RE (1984) Neural crest cell behavior in white and dark larvae of *Ambystoma mexicanum*: differences in cell morphology, arrangement and extracellular matrix as related to migration. J Exp Zool 229:91–107

Stigson M (1996) Large chondroitin sulfate proteoglycans in the axolotl embryo. Thesis, Uppsala University, Uppsala, Sweden

Stigson M, Kjellén L (1991) Large disulfide-stabilized proteoglycan complexes are synthesized by the epidermis of axolotl embryos. Arch Biochem Biophys 290:391–396

Stigson M, Löfberg J, Kjellén L (1997a) PG-M/versican-like proteoglycans are components of large disulfide-stabilized complexes in the axolotl embryo. J Biol Chem 272:3246–3253

Stigson M, Löfberg J, Kjellén L (1997b) Reduced epidermal expression of a PG-M/versican-like proteoglycan in embryos of the white mutant axolotl. Exp Cell Res 236:57–65

Tajima Y, Moore MAS, Soares V, Ono M, Kissel H, Besmer P (1998) Consequences of exclusive expression in vivo of kit-ligand lacking the major proteolytic cleavage site. Proc Natl Acad Sci USA 95:11903–11908

Thibaudeau G, Frost-Mason SK (1992) Inhibition of neural crest cell differentiation by embryo ectodermal extract. J Exp Zool 261:431–440

Toksoz D, Zsebo KA, Smith S, Hu D, Brankow D, et al (1992) Support of human hematopoiesis in long-term none marrow culutres by murine stromal cells selectively expressing the membrane-bound and secreted forms of the human homolog of the steel gene product, stem cell factor. Proc Natl Acad Sci USA 89:7350–7354

Tsukahara T, Okimura M, Suzuki S, Iwata H, Miura T, Kimata K (1991) Enhanced expression of fibronectin by *cmd/cmd* chondrocytes and its modulation by exogenously added proteoglycan. J Cell Sci 100:387–395

Voss SR (1995) Genetic basis of paedomorphosis in the axolotl, *Ambystoma mexicanum*: a test of the single-gene hypothesis. J Hered 86:441–447

Voss SR, Shaffer HB (1996) What insights into the developmental traits of urodeles does the study of interspecific hybrids provide? Int J Dev Biol 40:885–893

Voss SR, Shaffer HB (1997) Adaptive evolution via a major gene effect: paedomorphosis in the Mexican axolotl. Proc Natl Acad Sci USA 94:14185–14189

Wehrle-Haller B, Weston JA (1995) Soluble and cell-bound forms of steel factor activity play distinct roles in melanocyte precursor dispersal and survival on the lateral neural crest migration pathway. Development 121:731–742

Wight TN, Kinsella MG, Qwarnström EE (1992) The role of proteoglycans in cell adhesion, migration and proliferation. Curr Opin Cell Biol 4:793–801

Yamagata M, Suzuki S, Akiyama SK, Yamada KM, Kimata K (1989) Regulation of cell-substrate adhesion by proteoglycans immobilized on extracellular substrates. J Biol Chem 264: 8012–8018

Zhang Z, Anthony RV (1994) Porcine stem cell factor/c-kit ligand: its molecular cloning and localization within the uterus. Biol Reprod 50:95–102

Zhou JH, Ohtaki M, Sakurai M (1993) Sequence of a cDNA encoding chicken stem cell factor. Gene 127:269–270

Zimmer A, Zimmer AM, Reynolds K (1994) Tissue specific expression of the retinoic acid receptor-β2: regulation by short open reading frames in the 5′-noncoding region. J Cell Biol 127:1111–1119

Zsebo KM, Williams DA, Geissler EN, Broudy VC, Martin FH, Atkins HL, Hsu R-Y, Birkett NC, Okino KH, Murdock DC, Jacobsen FW, Langley KE, Smith KA, Takeishi T, Cattanach BM, Galli J, Suggs SV (1990) Stem cell factor is encoded at the *Sl* locus of the mouse and is the ligand of the c-*kit* tyrosine kinase receptor. Cell 63:213–224

Zubiaga AM, Belasco JG, Greenberg ME (1995) The nonamer UUAUUUAUU is the key AU-rich sequence motif that mediates mRNA degradation. Mol Cell Biol 15:2219–2230